

Supplemental Information

Detailed Experimental Procedures:

***O. carmela*, Illumina library construction**

A paired-end genomic library for Illumina sequencing was constructed using *Oscarella carmela* DNA prepared by whole genome amplification (WGA, (1)). To reduce contamination and polymorphism that could complicate genome assembly and analysis, a single sponge larva was isolated, washed five times in sterile-filtered seawater and lysed using the REPLI-g Mini kit for WGA (Qiagen, Valencia, CA). The lysate was divided and used to conduct four separate WGA reactions that were pooled to reduce the effects of stochastic amplification bias. Paired-end library construction was performed using the Illumina PE Adapter Oligo Mix and PCR primers (Illumina Inc., San Diego, CA) in combination with protocol modifications suggested by Quail and colleagues (2). Additionally, during each spin-column purification step, residual ethanol was pipetted out of the column prior to elution to prevent ethanol carry-over. Library quality was determined using a 2100 Bioanalyzer (Agilent Technologies, Santa Clara, CA) to confirm fragment size and concentration.

***O. carmela* Illumina sequencing and draft genome assembly**

A total of 388,627,652 reads were generated from two separate paired-end Illumina runs on the same library: 39,460,320 reads from 2 lanes of 76 cycle sequencing (hereafter called “run 1”), and 349,167,332 reads from 7 lanes of 101 cycle sequencing (“run 2”). Before assembly, low frequency “noise” k-mers were corrected in the reads using the Corrector tool version 1.00 from the Beijing Genomics Institute [<http://soap.genomics.org.cn/down/correction.tar.gz>] with default parameter values. The two lanes from run 1 were corrected together using a frequency cutoff of 5 per k-mer, and each lane from run 2 was corrected individually using a frequency cutoff of 10 per k-mer. After correction, 33,249,809 reads from run 1 and 298,166,837 reads from run 2 remained, for a total of 331,416,646 reads. Genome assembly was performed iteratively using

SOAPdenovo version 1.04 (3) with default parameter values (unless otherwise noted), as follows: an initial assembly was created using a k-mer size of 31, with both runs used for building contigs and only run 1 used for building scaffolds. To close gaps in the initial assembly, we ran GapCloser version 1.10 (4) with default parameter values using only reads from run 1. We found that the processes of building scaffolds and gap closing were more successful using fewer reads, and thus we chose run 1 for both tasks; using the reads from any single lane of run 2 produced similar results. After running SOAPdenovo and GapCloser, we mapped all corrected reads back to the assembly using Bowtie version 0.12.1 (5) with default parameter values. We then created a final assembly using only the reads that mapped to the initial gap-closed assembly. We ran SOAPdenovo followed by GapCloser, repeating the initial assembly process but instead using at each step the set of reads mapping to the initial assembly. Assembly statistics are shown in Tables S1-S3.

***O. carmela* gene prediction**

Gene prediction was performed *de novo* on the final assembly using Augustus version 2.3 (6) with the autoAug script and the 6,235 assembled Sanger ESTs (7) as prediction aids. Gene prediction was only performed on sequences with a minimum length of 500 (9,823 genes were predicted).

O. carmela genome: assembly statistics for scaffolds

| Assemblies | Number of Scaffolds | Total Assembly Size (bp) | Number of Scaffolds + Contigs | Longest (bp) | N50 (bp) | N90 (bp) |
|------------------|---------------------|--------------------------|-------------------------------|--------------|----------|----------|
| Pilot assembly | 29,148 | 57,006,393 | 70,595 | 49,630 | 3,324 | 416 |
| Initial assembly | 22,699 | 60,727,654 | 77,270 | 84,460 | 4,699 | 351 |
| Final assembly | 17,451 | 56,386,309 | 67,767 | 108,178 | 5,897 | 368 |

O. carmela genome: assembly statistics for contigs

| Assemblies | Number of Reads | Total Assembly Size (bp) | Longest (bp) | N50 (bp) | N90 (bp) | Average Coverage (x) |
|------------------|-----------------|--------------------------|--------------|----------|----------|----------------------|
| Pilot assembly | 39,460,320 | 46,779,956 | 6,153 | 339 | 124 | 22 |
| Initial assembly | 331,416,646 | 54,313,237 | 28,111 | 890 | 132 | 568 |
| Final assembly | 239,209,057 | 54,193,990 | 43,946 | 1,158 | 142 | 562 |

O. carmela genome: scaffold GC content, paired end insert size, and gap information

| Assemblies | GC Content (percent) | Estimated Insert Size (bp) | Estimated Insert Standard Deviation (bp) | Number of Gaps Before GapCloser | Total Size of Gaps Before GapCloser (bp) | Number of Gaps Remaining After GapCloser | Total Size of Gaps Remaining After GapCloser (bp) |
|------------------|----------------------|----------------------------|--|---------------------------------|--|--|---|
| Pilot assembly | 43.7 | 390 | 78 | 85,376 | 13,410,978 | - | - |
| Initial assembly | 43.5 | 397 | 71 | 55,768 | 7,991,639 | 21,580 | 5,733,376 |
| Final assembly | 43.5 | 395 | 79 | 39,994 | 4,765,458 | 8,105 | 2,452,188 |

Discovery and annotation of novel cadherins

The stand-alone BLAST search algorithm was used to search the best predicted protein set from the draft genomes of *S. rosetta*, *C. owczarzaki*, and *O. carmela* using the 23 predicted cadherins from the *M. brevicollis* genome (8) as a query. As a complement to this approach, Pfam (9), SMART (10) and Phobius (11) domain prediction programs were run on all predicted *S. rosetta* proteins. Every protein predicted to have at least one extracellular cadherin (EC) domain was annotated and categorized according to whether its overall domain composition and architecture matched known cadherins from *M. brevicollis* or any metazoan. The *S. rosetta* gene models are supported by 33-fold sequence coverage suggesting that we have identified most, if not all cadherins in the genome (12). Accurate abundance data for *O. carmela* could not be determined due to the

early draft status of the genome. Therefore, cadherin abundance in sponges was determined from the genome of *Amphimedon queenslandica* (11). Cadherin abundance estimates for eumetazoans were derived from Hulpiou and van Roy (13) and references therein. Taxonomic data from SMART were used to conclude that no EC domains are present in any annotated plant or fungus.

HMM searches for Hh-N domain-containing proteins

We used the HMMER 3.0 suite of tools (14) to build custom models of the Hh-N signaling domain in order to increase sensitivity for searches of choanoflagellates and other opisthokonts. We used *hmmsearch* (14) with the Pfam domain Hh_signal [PF01085, Pfam version 24.0 (9)] to detect Hh-N domains in the predicted protein sets from the genomes of the sponge *A. queenslandica* (15), the sea anemone *N. vectensis* (16), and the choanoflagellates *S. rosetta* (12) and *M. brevicollis* (17). Using the sequences of all domains predicted by *hmmsearch* with an E value below the gathering threshold for the model in Pfam, we built a multiple alignment using the FSA web server version 1.15.2 (18). We used the resulting alignment to build a custom model with *hmmbuild* (14), and ran *hmmsearch* with the custom model against the predicted protein sets from *O. carmela*, *S. rosetta* and *M. brevicollis* in order to detect previously unidentified instances of the Hh-N domain.

Cloning full-length Ocar_bcat

Tissue of *O. carmela* was flash frozen and ground to a powder using a mortar and pestle containing liquid nitrogen. Messenger RNA was isolated using Trizol Reagent (Invitrogen Corp., Carlsbad, CA) followed by the Oligotex mRNA Mini Kit (Qiagen, Valencia, CA). The unknown 5' sequence of Ocar_bcat was cloned and sequenced using GeneRacer (Invitrogen Corp., Carlsbad, CA) in combination with an antisense primer (SN33R: 5' CCCAAGGGCAAGTCTTCGCTGGAT 3') corresponding to the known 3' EST sequence (7). The full-length sequence is deposited in GenBank (HQ234356).

Ocar_bcat structural predictions

The full-length sequence of Ocar_bcat was translated from the cloned mRNA transcript using NCBI ORF Finder. The predicted protein was analyzed for its homology to known beta-catenin sequences by comparing its primary sequence to the non-redundant Genbank database (nr) via blastp (19) and by searching for conserved structural domains (arm repeats) using Pfam (9) and SMART (10). Each predicted arm repeat in beta-catenin-related proteins from human, *O. carmela*, *M. brevicollis*, *S. rosetta*, *Dictyostelium discoideum* and *Arabidopsis thaliana* was subjected to pair-wise reciprocal blast (9). For example, arm repeat 1 from Ocar_bcat was used to perform a Blastp (19) search against a database of all arm repeats from all sampled proteins. We expected that orthologous sequences from different species would exhibit a co-linear sequence of arm repeat homology with human beta-catenin [Fig.S5; method modified from (20)]. In the example of *O. carmela* arm repeat 1, only a best-reciprocal blast with arm repeat 1 from human beta-catenin would be interpreted support homology of these two proteins.

To identify conserved functional residues and motifs within Ocar_bcat, multiple sequence alignment was performed using MUSCLE (21). Additionally, the three-dimensional structure of Ocar_bcat was analyzed using alignment-based fold-prediction as implemented by LOOPP (22). Predicted structures were visualized with PyMOL (The PyMOL Molecular Graphics System, Version 1.2r3pre, Schrödinger, LLC.).

Yeast two-hybrid screen

A yeast two-hybrid screen was conducted to identify candidate binding-partners of full-length Ocar_bcat. To construct a yeast expression library representative of the expressed genes of *O. carmela*, mRNA was isolated from pooled adult and embryonic tissues (from many individuals to maximize transcript diversity) and cloned into pDONR222 using the CloneMiner cDNA Library Construction Kit (Invitrogen Corp., Carlsbad, CA). Inserts from this library were shuttled into the

yeast two-hybrid prey plasmid, pDEST22 using LR Clonase II enzyme mix (Invitrogen Corp., Carlsbad, CA) and transformed for storage and amplification into ElectroMAX DH10B T1 Phage Resistant Cells (Invitrogen Corp., Carlsbad, CA). Likewise, full-length Ocar_bcat was modified using PCR to incorporate Gateway compatible attB1/attB2 recombination sites and cloned into pDONR221 using BP Clonase II enzyme mix (Invitrogen Corp., Carlsbad, CA). This insert was shuttled into the yeast two-hybrid bait-plasmid, pDEST32 using LR Clonase II enzyme mix.

Yeast transformation and screening was performed at the yeast two-hybrid facility at Indiana University (23). Full-length Ocar_bcat and positive clones were tested for autoactivation on his- media. E-Amino-1,2,4-Triazol (3AT), which acts as a quantitative inhibitor of the HIS3 reporter gene, was used to control autoactivation by Ocar_bcat. After a <10 day screen, positive clones were retested on his- media, ura- media, and in LacZ assays. Inserts from positive clones were rescued and sequenced at the University of California DNA sequencing facility. Insert sequences from positive clones were compared against the draft assembly of the *O. carmela* genome using blastn (19) and predicted proteins were annotated using blastp (19), Pfam (9) and SMART (10) to test for homology with known proteins.

Seventeen unique candidate binding-partners of Oc_bcat were detected (Table S2), including three clones encoding the CCD region of OcCdh1 and an additional well-known beta-catenin binding protein, Axin. These detected interactions could not be independently validated using in vitro binding assays because recombinant forms of Ocar_bcat proved to be highly insoluble. Nevertheless, the conserved structural features of Ocar_bcat and Ocar_Cdh1, coupled with the fact that this is a widely conserved interaction in metazoans, suggest that the yeast two-hybrid result represents a *bona fide* interaction.

Fig. S1

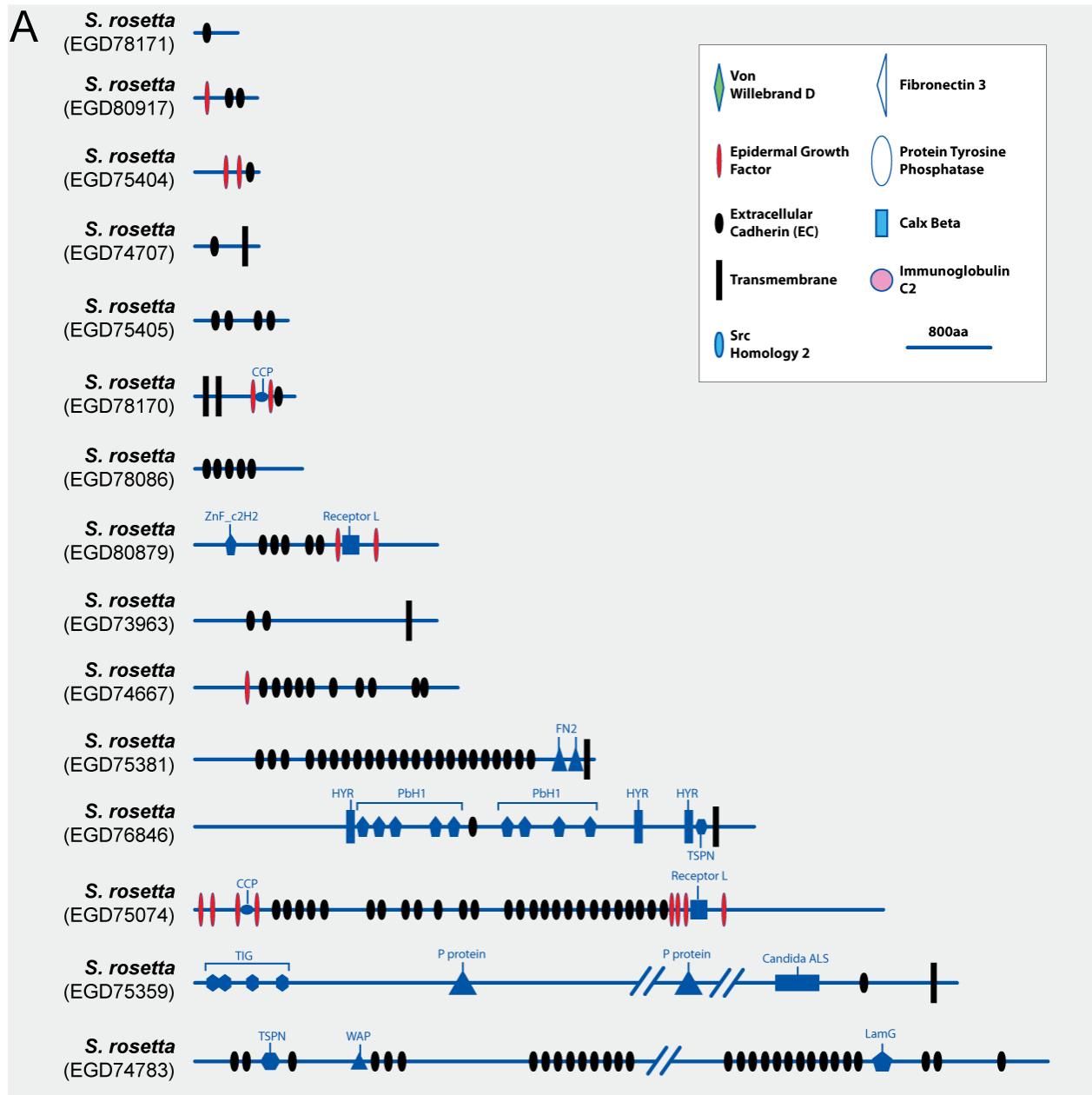


Fig. S1, continued.

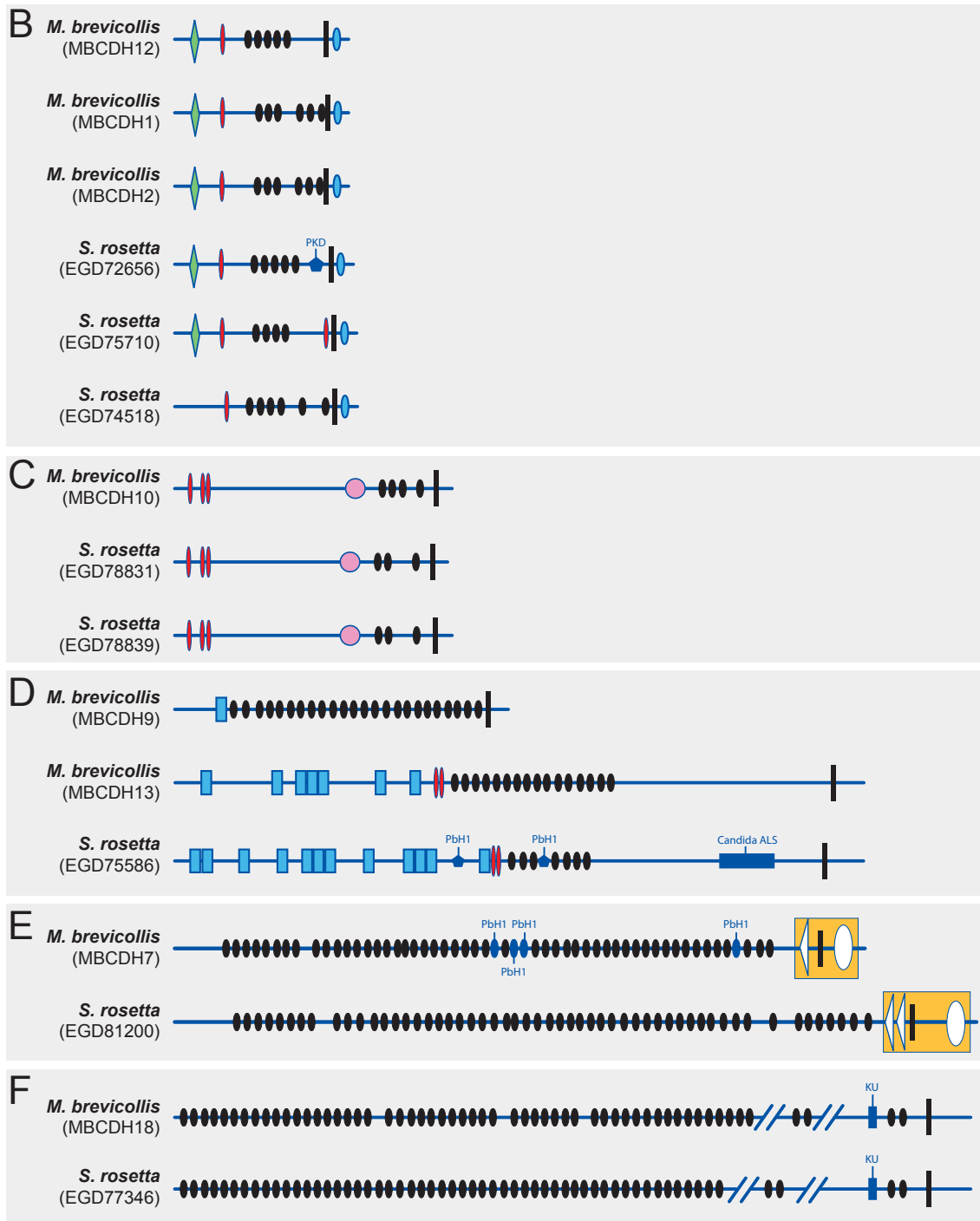


Fig. S1. Domain architecture of *S. rosetta* cadherins without orthologs in Metazoa or *C. owczarzaki*. (A) 16 out of 29 predicted *S. rosetta* cadherin proteins have no clear orthology to any cadherins known from other species,

whereas five protein families (B-F) can be identified as shared between and exclusive to *S. rosetta* and *M. brevicollis* based upon similarities in their domain composition and arrangement. Of these, one family (E) has partial homology to the lefftyrin family that is found in choanoflagellates and sponges. However, genes in this family differ from choanoflagellate lefftyrins in that they are predicted to have catalytically active cytoplasmic PTPase domains.

(Abbreviations: Candida ALS = Candida Agglutinin-like sequence; CCP = domain abundant in complement control proteins; FN2 = fibronectin 2; HYR = Hyalin Repeat; KU = BPTI/Kunitz family of serine protease inhibitors; LamG = laminin G domain; P protein = Proprotein convertase P-domain; PbH1 = parallel beta-helix repeats; PKD = polycystic kidney disease; TIG = transcription factor immunoglobulin-like domain; TSPN = Thrombospondin N-terminal-like domain; WAP = whey acidic protein; ZnF_c2h2 = zinc-finger, c2h2 type).

Fig. S2.

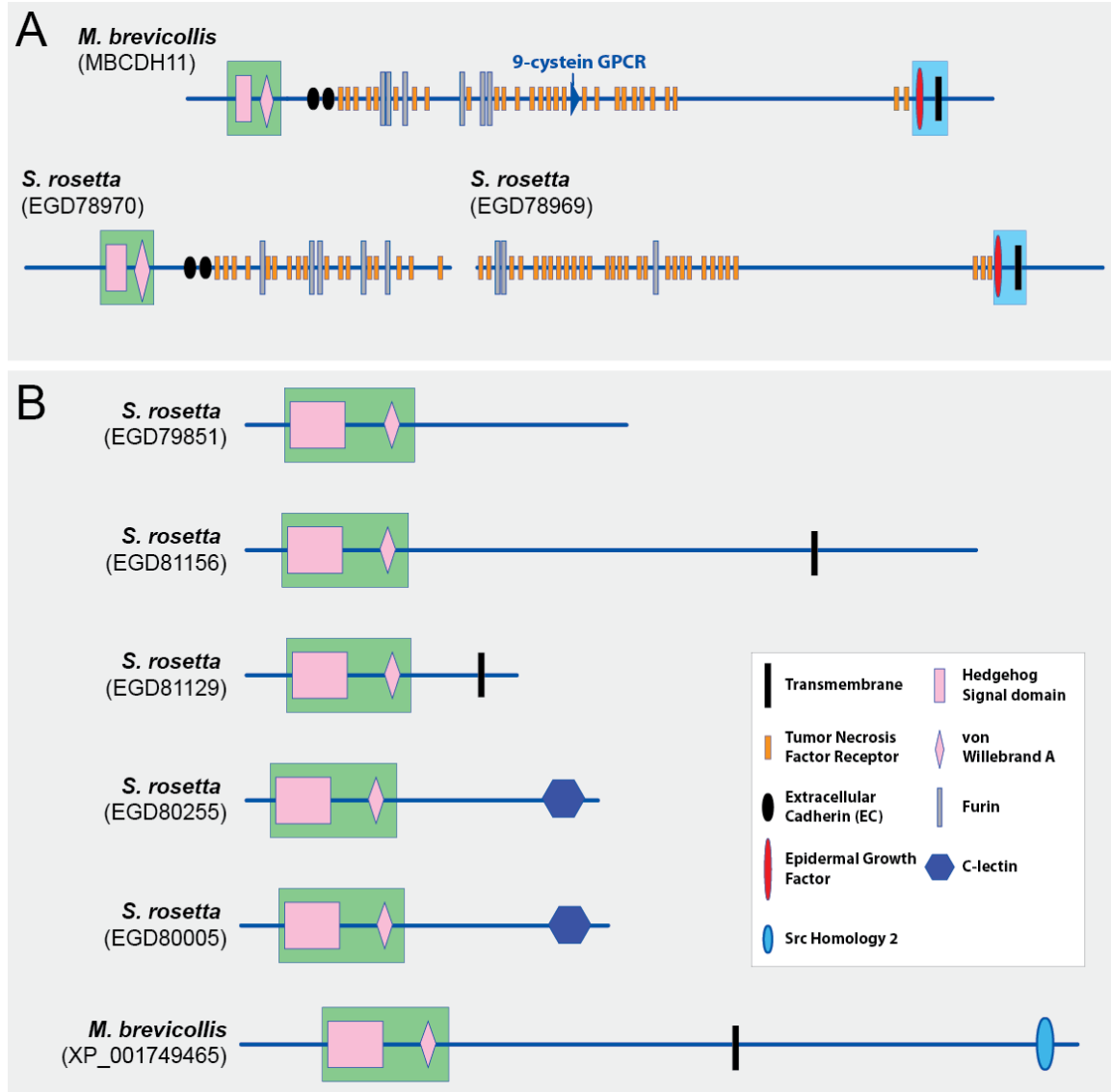


Fig. S2. Additional detected Hh-N domain containing proteins from *S. rosetta* and *M. brevicollis*. (A) In *S. rosetta*, two adjacent gene models on a single scaffold have close homology to parts of *M. brevicollis* hedgling (MBCDH11). Both gene models are supported by RNAseq expression data, but there is a predicted stop codon between them and there are no RNAseq reads that span the divide. We infer either that the stop codon that splits *S. rosetta* hedgling evolved following the divergence of the *M. brevicollis* and *S. rosetta* lineages, or that it is the result of a genome assembly error. Further interpretation

will require experimental investigation of these gene models. (B) Using a custom HMM created against the Hh-N domain of known hedgling proteins we also identified five *S. rosetta* proteins and one *M. brevicollis* protein that have a conserved Hh-N domain, but lack EC domains. In each case, as in all known hedglings, the Hh-N domain is adjacent to a von Willebrand A domain. Therefore, we hypothesize that the association of these two domains in diverse proteins and in diverse organisms reflects an ancestral function that has been lost in eumetazoans.

Fig. S3

| | | | | | | | | | | | | | | | | | | | | | | | | | | | | | | | | | | |
|-------------|---|---|---|---|---|---|---|---|---|---|---|---|---|---|---|---|---|---|---|---|---|---|---|---|---|---|---|---|---|---|---|---|---|---|
| Pfam HMM | e | v | k | i | g | k | v | s | a | a | v | G | d | t | v | t | v | p | V | t | v | k | n | v | p | k | k | . | v | a | g | a | q | |
| MBCDH8 (1) | . | . | . | . | . | . | . | . | . | A | I | G | D | T | F | T | V | P | V | R | V | N | A | G | S | S | T | . | L | A | S | I | D | |
| MBCDH8 (2) | . | . | . | . | . | . | . | . | . | A | I | G | D | T | F | T | V | P | V | R | V | N | A | G | S | S | T | . | L | A | S | I | D | |
| EGD82245 | . | . | . | . | . | . | . | . | . | . | . | . | . | . | . | . | V | N | V | Y | V | N | T | G | S | L | V | . | L | G | G | V | D | |
| Aqu1.221884 | . | . | . | . | . | . | . | . | . | . | . | . | . | . | . | D | V | P | V | R | V | N | I | G | K | N | N | L | L | D | A | I | E | |
| Pfam HMM | f | t | i | k | Y | D | p | a | v | L | e | v | v | s | v | t | a | G | s | l | i | v | q | k | n | p | n | s | s | f | s | a | n | |
| MBCDH8 (1) | L | S | V | Y | Y | D | P | S | R | L | E | A | V | S | V | A | P | G | S | A | W | . | . | P | S | S | A | Q | L | T | A | T | | |
| MBCDH8 (2) | L | S | V | Y | Y | D | P | S | R | L | E | A | V | S | V | A | P | G | S | A | W | . | . | P | S | S | A | Q | L | T | A | T | | |
| EGD82245 | L | E | V | Y | Y | D | A | S | I | V | E | P | V | D | V | V | P | G | A | . | . | . | T | W | P | G | G | T | F | V | K | T | | |
| Aqu1.221884 | L | A | V | G | Y | D | S | S | S | L | S | L | L | S | V | S | P | G | S | D | W | . | . | . | E | G | D | W | F | S | N | S | | |
| Pfam HMM | v | d | e | n | k | g | i | i | k | f | l | f | l | d | d | t | y | g | s | s | g | i | a | e | d | . | G | v | f | a | t | i | t | |
| MBCDH8 (1) | L | D | D | P | P | G | V | V | L | F | G | . | . | G | A | L | D | T | T | G | L | Q | G | T | . | K | E | I | A | V | L | T | | |
| MBCDH8 (2) | L | D | D | P | P | G | V | V | L | F | G | . | . | G | A | L | D | T | T | G | L | Q | G | T | . | K | E | I | A | V | L | T | | |
| EGD82245 | L | N | D | P | V | G | T | I | L | L | G | . | . | G | . | V | T | E | D | G | I | A | S | T | S | Y | H | L | A | T | I | Q | | |
| Aqu1.221884 | L | T | Y | Y | D | G | F | V | H | F | G | . | . | G | V | L | S | T | S | . | I | S | G | I | . | A | E | V | A | V | L | R | | |
| Pfam HMM | f | k | V | k | s | a | a | a | t | g | i | t | t | a | v | s | i | s | s | l | f | v | f | d | . | d | e | t | l | k | e | i | s | |
| MBCDH8 (1) | F | R | V | L | A | G | A | T | V | G | Q | R | L | A | L | T | G | Q | V | T | T | M | A | D | T | D | G | V | L | M | G | A | E | |
| MBCDH8 (2) | F | R | V | L | A | G | A | T | V | G | Q | R | L | A | L | T | G | Q | V | T | T | M | A | D | T | D | G | V | L | M | G | A | E | |
| EGD82245 | F | Q | V | V | . | . | . | . | . | . | . | . | . | . | . | . | . | . | . | . | . | . | . | . | . | . | . | . | . | . | . | . | . | . |
| Aqu1.221884 | F | R | A | Q | S | N | Q | . | . | . | . | . | . | . | . | . | . | . | . | . | . | . | . | . | . | . | . | . | . | . | . | . | . | |
| Pfam HMM | v | v | t | a | v | d | g | s | v | t | v | | | | | | | | | | | | | | | | | | | | | | | |
| MBCDH8 (1) | N | R | A | F | V | A | G | S | V | E | | | | | | | | | | | | | | | | | | | | | | | | |
| MBCDH8 (2) | N | R | A | F | V | A | G | S | V | E | | | | | | | | | | | | | | | | | | | | | | | | |
| EGD82245 | . | . | . | . | . | . | . | . | . | . | | | | | | | | | | | | | | | | | | | | | | | | |
| Aqu1.221884 | . | . | . | . | . | . | . | . | . | . | | | | | | | | | | | | | | | | | | | | | | | | |

Fig. S3. Cohesin domains from Coherin family proteins aligned against the Cohesin Hidden Markov Model from Pfam. Residues that exactly match Pfam HMM (highlighted in blue) are indicated with black shading whereas residues that are considered to be a conservative substitution with respect to what the model expects are indicated with gray shading. Cohesin domains 1 and 2 from *Monosiga brevicollis* (MBCDH8) are identical to each other. Protein identifiers correspond to Fig. 2c. (Abbreviations: HMM: Hidden Markov Model).

Fig. S4

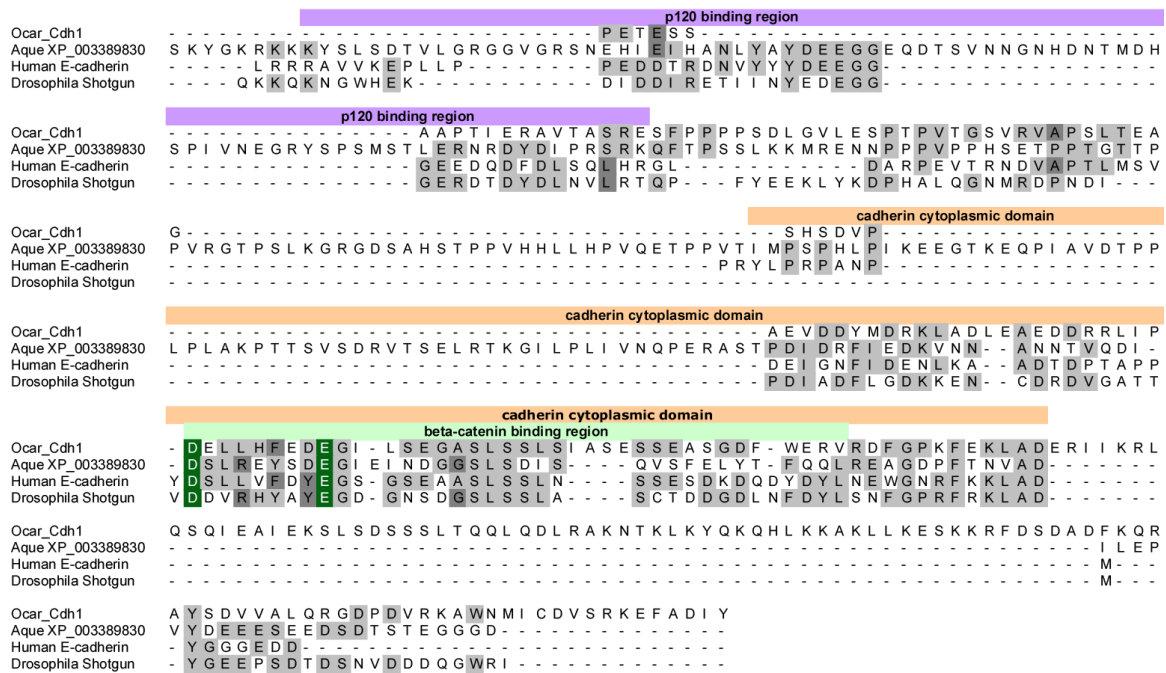


Fig. S4. Annotated alignment of classical cadherin cytoplasmic tails. The juxtamembrane domain (purple box) that constitutes the binding site for p120 catenin is partially conserved between human and *Drosophila* and *Amphimedon*, but is divergent in Ocar_Cdh1. In contrast, the beta-catenin binding domain (light green box) of the predicted CCD (light orange box) of Ocar_Cdh1 is conserved, including at residues that are required for the interaction (dark green). The sponge sequences are predicted to be longer than their bilaterian counterparts, complicating alignment of all but the most highly conserved residues.

Fig. S5.

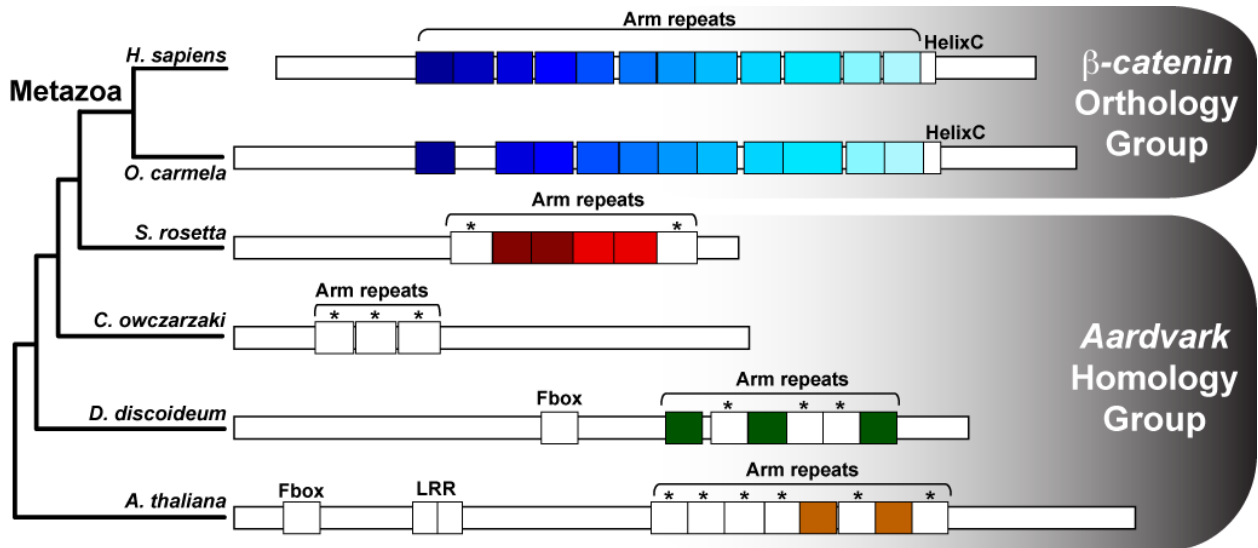


Fig. S5. Domain organization and phylogenetic distribution of proteins with homology to beta-catenin.

Protein diagrams are mapped onto a previously determined phylogenetic tree (24) with arm domains colored to indicate their similarity. Repeats of the same color are best-reciprocal Blast pairs. Arm repeats without close identity to any other are uncolored and indicated with an asterisk. Linear conservation of homologous arm repeats is restricted to metazoan beta-catenin orthologs, suggesting that the metazoan roles of beta-catenin evolved in the metazoan stem lineage and have been highly conserved throughout metazoan evolution.

Tables.

Table S1. *S. rosetta* cadherin expression levels.

| Genbank ID | Min FPKM¹ | Max FPKM | Mean FPKM | Median FPKM |
|-------------------|-----------------------------|-----------------|------------------|--------------------|
| EGD80879 | 27.617977 | 113.246096 | 56.93163613 | 48.3590645 |
| EGD80917 | 2.25581 | 6.049739 | 3.860855875 | 3.533781 |
| EGD78831 | 7.874201 | 40.03944 | 19.4444355 | 15.1492895 |
| EGD78839 | 0.109114 | 26.26796 | 11.104367 | 9.8600525 |
| EGD79002 | 1.87756 | 6.256101 | 3.839630625 | 3.370277 |
| EGD79017 | 29.325694 | 128.553899 | 80.03320963 | 89.619573 |
| EGD82245 | 3.403667 | 15.877104 | 9.775254375 | 10.434421 |
| EGD82557 | 0.85664 | 8.627106 | 4.377121 | 3.1091385 |
| EGD72656 | 168.694501 | 984.67225 | 624.6796178 | 621.626123 |
| EGD73963 | 2.017099 | 8.457588 | 4.626551625 | 3.828202 |
| EGD74518 | 46.138224 | 267.075716 | 159.4101904 | 161.7252545 |
| EGD74707 | 1.962277 | 15.002993 | 8.222477875 | 8.487063 |
| EGD75381 | 0.133699 | 51.162787 | 18.63580838 | 15.35265 |
| EGD75404 | 3.990599 | 9.91731 | 7.319792125 | 7.684626 |
| EGD75405 | 2.37142 | 9.804725 | 6.56574025 | 6.3694265 |
| EGD75586 | 0.087914 | 6.21004 | 2.840604125 | 2.17229 |
| EGD75074 | 2.197013 | 6.533185 | 4.66290875 | 4.722256 |
| EGD74783 | 0.026136 | 3.799631 | 1.556376 | 1.0930275 |
| EGD75710 | 71.962177 | 626.409101 | 259.4577603 | 220.060925 |
| EGD76846 | 5.967787 | 85.11871 | 33.87954975 | 17.35544 |
| EGD77346 | 7.357232 | 20.994633 | 12.16801713 | 10.4218215 |
| EGD78086 | 0 | 7.934519 | 2.76326325 | 1.801815 |
| EGD78170 | 18.746381 | 50.514396 | 28.3529975 | 26.7736315 |
| EGD78171 | 23.099038 | 61.605291 | 35.97480775 | 33.790346 |
| EGD81200 | 0.053023 | 20.10651 | 9.513880375 | 8.764376 |
| EGD78969 | 9.214266 | 59.752132 | 31.85870863 | 33.0626255 |
| EGD78970 | 5.89713 | 31.968329 | 15.953967 | 15.8754105 |
| EGD74667 | 2.071066 | 14.728778 | 7.26199325 | 6.9755495 |
| EGD75359 | 0.023944 | 7.275513 | 3.04185575 | 2.4945935 |
| EGD79249 | 0.020866 | 3.374047 | 1.3963085 | 1.166545 |

¹The number of fragments per kilobase per million sequenced reads (FPKM) mapping to each identified *S. rosetta* cadherin from RNA-seq of eight growth conditions is summarized as evidence of gene expression.

Table S2. *O. carmela* binding partners predicted from yeast two-hybrid screen of beta-catenin.

| gene ID | Tentative Identification | Predicted domain architecture (Pfam) | Predicted domain architecture (Smart) |
|-----------|---|--------------------------------------|---------------------------------------|
| g4908.t1 | none | none | none |
| g9583.t1 | none | death | none |
| g6098.t1 | Upstream binding protein | CP2 | none |
| g8349.t1 | 40S ribosomal protein S11 | Ribosomal S17 | none |
| g6246.t1 | Tenascin | EGF 2 (x9); EGF Ca (x2) | VWD; EGF like; EGF (x10); EGF Ca (x2) |
| g6719.t1 | none | EIF4E-T | coiled coil |
| g8701.t1 | Transcription factor AP-1/c-Jun | bZIP 1 | BRLZ |
| g2054.t1 | Calumenin | SPARC Ca bdg; efhand (x2) | EFh (x2) |
| g6285.t1 | E74-like factor | Ets | ETS |
| g10012.t1 | Chromosomal segregation protein SMC | none | coiled-coil |
| g4744.t1 | GTPase Rab2 | Ras | RAB |
| g8915.t1 | Baculoviral IAP repeat-containing protein 4 | BIR (x4) | BIR (x4); RING |
| g6056.t1 | Ribosomal protein L13 | Ribosomal L13e | none |
| g2979.t1 | Ral | Ras | RAS |
| g3724.t1 | Choline-phosphate cytidyltransferase | none | coiled-coil |
| g6554.t1 | Axin | RGS; DIX | RGS; DAX |
| AEC12441 | Ocar_Cdh1 | EC; EGF; Lam-G; CCD | EC; EGF; Lam-G |

References

1. Hosono S, *et al.* (2003) Unbiased whole-genome amplification directly from clinical samples. *Genome Res* 13(5):954-964.
2. Quail MA, *et al.* (2008) A large genome center's improvements to the Illumina sequencing system. *Nat Methods* 5(12):1005-1010.
3. Li R, *et al.* (2010) De novo assembly of human genomes with massively parallel short read sequencing. *Genome Res* 20(2):265-272.
4. <http://soap.genomics.org.cn/down/GapCloser.tar.gz>
5. Langmead B, Trapnell C, Pop M, & Salzberg SL (2009) Ultrafast and memory-efficient alignment of short DNA sequences to the human genome. *Genome Biol* 10(3):R25.
6. Stanke M, Diekhans M, Baertsch R, & Haussler D (2008) Using native and syntenically mapped cDNA alignments to improve de novo gene finding. *Bioinformatics* 24(5):637-644.
7. Nichols SA, Dirks W, Pearse JS, & King N (2006) Early evolution of animal cell signaling and adhesion genes. *Proc Natl Acad Sci U S A* 103(33):12451-12456.
8. Abedin M & King N (2008) The premetazoan ancestry of cadherins. *Science* 319(5865):946-948.
9. Finn RD, *et al.* (2010) The Pfam protein families database. *Nucleic Acids Res* 38(Database issue):D211-222.
10. Schultz J, Milpetz F, Bork P, & Ponting CP (1998) SMART, a simple modular architecture research tool: identification of signaling domains. *Proc Natl Acad Sci U S A* 95(11):5857-5864.
11. Kall L, Krogh A, & Sonnhammer EL (2007) Advantages of combined transmembrane topology and signal peptide prediction--the Phobius web server. *Nucleic Acids Res* 35(Web Server issue):W429-432.
12. http://www.broadinstitute.org/annotation/genome/multicellularity_project/MultiHome.html
13. Hulpiau P & van Roy F (2011) New insights into the evolution of metazoan cadherins. *Mol Biol Evol* 28(1):647-657.
14. <http://www.hmmmer.janelia.org>
15. Srivastava M, *et al.* (2010) The *Amphimedon queenslandica* genome and the evolution of animal complexity. *Nature* 466(7307):720-726.
16. Putnam NH, *et al.* (2007) Sea anemone genome reveals ancestral eumetazoan gene repertoire and genomic organization. *Science* 317(5834):86-94.
17. King N, *et al.* (2008) The genome of the choanoflagellate *Monosiga brevicollis* and the origin of metazoans. *Nature* 451(7180):783-788.
18. Bradley RK, *et al.* (2009) Fast statistical alignment. *PLoS Comput Biol* 5(5):e1000392.
19. Altschul SF, *et al.* (1997) Gapped BLAST and PSI-BLAST: a new generation of protein database search programs. *Nucleic Acids Res* 25(17):3389-3402.
20. Oda H, Tagawa K, & Akiyama-Oda Y (2005) Diversification of epithelial adherens junctions with independent reductive changes in cadherin form: identification of potential molecular synapomorphies among bilaterians. *Evol Dev* 7(5):376-389.

21. Edgar RC (2004) MUSCLE: multiple sequence alignment with high accuracy and high throughput. *Nucleic Acids Res* 32(5):1792-1797.
22. Tobi D & Elber R (2000) Distance-dependent, pair potential for protein folding: results from linear optimization. *Proteins* 41(1):40-46.
23. http://sites.bio.indiana.edu/~michaelslab/yeast_two_hybrid_facility.html
24. Ruiz-Trillo I, Roger AJ, Burger G, Gray MW, & Lang BF (2008) A phylogenomic investigation into the origin of metazoa. *Mol Biol Evol* 25(4):664-672.